Cell mediated immune response of the Mediterranean sea urchin *Paracentrotus lividus* after PAMPs stimulation.

A Romero, B Novoa, A Figueras *

Marine Research Institute - CSIC. Eduardo Cabello 6, 36208 Vigo, Spain.

*Corresponding author:

Tlf: 34 986 21 44 63

Fax 34 986 29 27 62

E-mail: antoniofigueras@iim.csic.es

aromero@iim.csic.es, virus@iim.csic.es

Submitted to: DCI

January 2016

Abstract

The Mediterranean sea urchin (*Paracentrotus lividus*) is of great ecological and economic importance for the European aquaculture. Yet, most of the studies regarding echinoderm´s immunological defense mechanisms reported so far have used the sea urchin *Strongylocentrotus purpuratus* as a model, and information on the immunological defense mechanisms of *Paracentrotus lividus* and other sea urchins, is scarce. To remedy this gap in information, in this study, flow cytometry was used to evaluate several cellular immune mechanisms, such as phagocytosis, cell cooperation, and ROS production in *P. lividus* coelomocytes after PAMP stimulation. Two cell populations were described. Of the two, the amoeboid-phagocytes were responsible for the phagocytosis and ROS production. Cooperation between amoeboid-phagocytes and non-adherent cells resulted in an increased phagocytic response. Stimulation with several PAMPs modified the phagocytic activity and the production of ROS. The premise that the coelomocytes were activated by the bacterial components was confirmed by the expression levels of two cell mediated immune genes: LPS-Induced TNF-alpha Factor (LITAF) and macrophage migration inhibitory factor (MIF). These results have helped us understand the cellular immune mechanisms in *P. lividus* and their modulation after PAMP stimulation.

Keywords:

Sea urchin; *P. lividus;* immune response; coelomocytes; flow cytometry; gene expression.

1. Introduction

Echinodermata is an ancient phylum of marine invertebrates which includes approximately 7000 living species and about 13,000 extinct species according to the fossil record. It is the largest phylum that does not include freshwater or terrestrial species (Brusca and Brusca, 2003). Echinoderms play a key role in the maintenance of seaweed communities by influencing the relative abundance of fish and other benthic invertebrates (Hereu et al., 2005; Guidetti and Dulcić, 2007). Among the echinoderms some species of sea urchins, such as the Chilean *Loxechinus albus* and several species of the genus *Strongylocentrotus*, are also important for their economic value in aquaculture (Andrew et al., 2002). In Europe, *Paracentrotus lividus* is distributed throughout the Mediterranean Sea and in the North-Eastern Atlantic Sea, from Scotland and Ireland to Southern Morocco and the Canary Islands (Andrew et al., 2002; Boudouresque and Verlaque, 2001). These species have a high commercial value in the sea food market because their gonads are considered a delicacy. Despite the wide distribution and potential economic relevance for the European aquaculture of *P. lividus,* few studies have been conducted to explain how this species interacts with pathogens and the cellular immune mechanisms it uses to overcome disease.

The immune system in echinoderms involves humoral and cellular components (Chia and Xing, 1996). The immune effector cells are a heterogeneous cell population called coelomocytes that move freely in all coelomic spaces (Smith et al., 2010). There is not a single standard classification of coelomocytes for all echinoderms since the cells are heterogeneous in morphology and size. Moreover, the cell type proportion varies with the species and the physiological conditions of each individual. Changes have been described in response to environmental factors, pollutants, pathogens or accidental injures (Matranga et al., 2000; Pinsino et al., 2007; Ramírez-Gómez et al., 2010). Based

on morphological criteria, coelomocytes have been classified into at least four cell types: amoebocytes, vibratile cells, and colourless and red spherule cells (Edds, 1993; Ramírez-Gómez and García-Arrarás, 2010; Deveci et al., 2015). The immune functions of each type of coelomocyte are still not totally understood, but it has been postulated that amoeboid-phagocytic cells and spherule cells are the only cellular components of the immune system (Ramírez-Gómez and García-Arrarás, 2010). Amoeboid-phagocytic cells share similar functional properties with vertebrate macrophages and granulocytes (Ito et al., 1992) as they are implicated in many immune processes such as encapsulation, aggregation, graft rejection (Matranga et al., 2000), phagocytosis and production of reactive oxygen and nitrogen species (ROS and NO, respectively) (Beck et al., 2001; Coteur et al., 2002b; Ito et al., 1992), inflammatory reactions (Smith et al., 2010), complement production (Gross et al., 1999), and antibacterial and cytotoxic activity (Haug et al., 2002; Lin et al., 2001). Cell cooperation between amoebocytes and spherulocytes has been reported to contribute to cell clumping (Canicattì and D'Ancona, 1989) and to the enhancement of the cytotoxic activity (Arizza et al., 2007a). The immune response can be induced by exposure to different pathogen-associated molecular patterns (PAMPs) such as lipopolysaccharide (LPS), b1-3-glucan or dsRNA (Terwilliger et al., 2007) and also to immunostimulants as chitosan, yeast polysaccharide, burdock oligosaccharide, seaweed polysaccharide, *Lentinus edodes* polysaccharide and poly (I: C) (Li et al., 2009).

Most of the immunological defense mechanisms in echinoderms have been described for the sea urchin *S. purpuratus* (Smith et al., 2010), and information in other sea urchins is scarce. Due to the wide diversity of species included in this taxonomic group, these results cannot be extrapolated to *P. lividus* without further research.

In the present study, we explored several cellular immune responses in the Mediterranean *P. lividus*. We used flow cytometry technology to evaluate cell cooperation, phagocytic activity and the production of ROS after stimulation with different PAMPs. Flow cytometry technology has been used for the classification and characterization of the coelomocytes in the starfish *Asterias rubens* and in the sea cucumber *Apostichopus japonicus* (Coteur et al., 2002a; Xing et al., 2008), but, to our knowledge, it is the first time it has been used in the Mediterranean sea urchin *P. lividus*. Moreover, neither the modulation of the phagocytic activity, nor the production of ROS and NO after treatment with different PAMPs, nor the expression of immune genes have been explored before in *P. lividus*.

2. Materials and Methods

2.1. Animals

Healthy sea urchins *Paracentrotus lividus* were collected at low tide from the intertidal zone on rocky beaches in Vigo (NW, Spain). Animals were transferred to 120 l fibre-glass tanks filled with filtered and aerated running sea water, and fed algae and mussels. The sea urchins were acclimatized for at least 1 week before the experiments.

2.2.Coelomic fluid collection

Perivisceral coelomic fluid (CF) was carefully collected from the oral region through the peristomal membrane. Up to 15 ml of the CF was drawn from a single animal using a sterile 1 ml syringe and a 25-gage needle. The needle was introduced diagonally to the peristomal coelom without perforating the gonads or the digestive

tube. To prevent clotting, coelomocytes were diluted 1:1 in an ice-cold solution (50mM 2-mercaptoethanol, 30 mM EDTA, pH 7.4) prepared in filtered seawater (FSW) (Bertheussen and Seijelid, 1978). In order to describe the different coelomocyte populations, 500 µl of CF (diluted 1:1 in anti-clotting solution) were placed on 8-wells culture slides (BD Falcon) and allowed to settle. After incubation at 15 ºC for 15 min, the supernatants were removed and the cells were observed under DIC microscopy using an Eclipse 80i light microscope (Nikon), and classified according to their size and morphology (Ramírez-Gómez and García-Arrarás, 2010). Digital micrographs were taken by a digital camera DXM 1200 (Nikon). Moreover, the cell concentration was calculated in a Neubauer chamber. Coelomocyte populations were defined by flow cytometry through the analysis of FSC-H /SSC-H density plots. Coelomocytes were analyzed immediately after the extraction (diluted 1:1 in anti-clotting solution) and after an incubation period of 1h at 15 ºC to enrich the samples with adherent cells. The non-adherent cells were almost totally removed by washing twice with 500 µl FSW. One hundred and fifty thousand cells were analysed in a FACSCalibur flow cytometer (Beckton and Dickinson).

2.3. Phagocytosis assay by flow cytometry

In all the experiments, the CF (diluted 1:1 in ice-cold anti-clotting solution) was incubated with one of the following fluorescein-labelled (FITC) particles (Molecular Probes): 1.3 µm latex beads, *E. coli* K-12 strain particles or zymosan A particles. The number of coelomocytes was estimated by counting cells in a Neubauer-counting chamber. Particles were added at a 100:1 particle:coelomocyte ratio. Control cells were incubated with FSW. After incubation in the dark at 15 °C for 2 hours, uninternalized

particles were removed by washing twice with 500 µl FSW. The attached cells were finally resuspended in 500 µl FSW using a rubber cell scraper. Fifty microliters of 0.4 % trypan blue solution (Sigma) in FSW were added to each sample to quench the fluorescence of adhered but non-phagocyted particles. One hundred and fifty thousand cells were analyzed in a FACSCalibur flow cytometer (BD). Phagocytosis was analysed in the whole cell population, and it was expressed as the percentage of cells that internalized at least one fluorescent particle (positive cells). Coelomocytes were observed using a Nikon Eclipse TS-100 fluorescent microscope, and photographed.

2.4. Cell cooperation between coelomocytes on the phagocytic activity

To analyse the influence that the presence of other cell types has in the phagocytic activity of the amoeboid-phagocytic cells, the phagocytic rates of samples enriched with adherent cells (amoebocytes) were compared with those obtained from whole coelomocyte preparations. In order to obtain samples enriched in amoebocytic cells (fractionated coelomocytes) the CF was dispensed into 24-wells cell culture plates (BD) and cells were allowed to settle and spread for 1 h at 15ºC. The non-adherent cells were removed by washing twice with 500 µl FSW. Cells were incubated with FITC-labeled particles at a 100:1 particle:coelomocyte ratio. Phagocytic activity of whole coelomocyte preparations was measured by mixing the FITC-labeled particles with the CF immediately after the extraction. The percentage of phagocytic cells that internalized at least one fluorescent particle was measured after 2 h of incubation as previously described. The experiment was repeated three times and 6 animals were used in each experiment.

2.5. Modulation of the phagocytic activity after PAMPs stimulation

Twelve mL of CF (diluted 1:1 in ice-cold anti-clotting solution) were extracted from one healthy sea urchin. The CFs (1 mL per sample) were mixed immediately after the extraction with FITC-labelled particles diluted in anti-clotting solution containing lipopolysaccharide (LPS, Sigma L2630), lipoteichoic acid (LTA, Sigma L2515), or polyinosinic:polycytidylic acid (Poly I:C, Sigma P9582) (at a final concentrations of 25 or 50 µg/mL). Controls were treated with FSW. Samples were dispensed into 24-wells cell culture plates (BD) and the phagocytic rates were measured after 2 h of incubation as previously described. The experiment was repeated three times and 6 animals were used in each experiment. Results were shown as the mean ± standard deviation of the percentage of cells that ingested at least one fluorescent particle. ANOVA followed by the Tukey multiple comparison test was carried out using the GraphPad Prism 5 software ($p<0.05$).

2.6. Production of Reactive Oxygen Species (ROS) and Nitric Oxide (NO) after PAMPs stimulation

The production of reactive oxygen species and nitrogen radicals was measured after cell stimulation with different PAMPs. Six animals were used in each experiment. Ten mL of CF were extracted from an individual sea urchin, diluted 1:1 in ice-cold anti-clotting solution and dispensed into 24-well cell culture plates (BD). After 30 min at 15 °C in the dark, the non-adhered cells were removed by washing twice with 500 µl FSW, and the remaining cells were incubated for 3 h at 15 ºC with 500 µl of different solutions containing LPS, LTA, Poly I:C, Zymosan A (Sigma Z4250) or Phorbol 12-myristate 13-acetate (PMA, Sigma) (at final concentration of 25 and 50 µg/mL).

The ROS production was analyzed by flow cytometry. After PAMP stimulation, cells were rinsed twice and 300 µl of FSW containing 0.4% DMSO and 5 µg/ml of the 2´,7´-dichlorodihydrofluorescein diacetate probe (H2DCF-DA, Molecular Probes) were added per well. Cells were incubated for 10 min on ice in the dark, washed twice and resuspended in 500 µl FSW. The percentage of cells producing oxygen radicals was measured by flow cytometry through the FL-1 channel. The mean fluorescence index was calculated as the ratio of stimulated samples to the control.

The concentration of extracellular NO_2^- radicals was quantified in the cell supernatants using a method based on the Griess reaction (Green et al., 1982). Briefly, after PAMP stimulation 50 µl of the supernatants were transferred to a new 96-well plate. One hundred µl of 1% sulphanilamide (Sigma) and other 100 µl of 0.1% N-naphthyl-ethylenediamine (Sigma) both prepared in 2.5% phosphoric acid were added to each well. The optical density (OD) was determined using a multiscan spectrophotometer (Labsystems) at 540 nm. The nitrite concentration (µM) in the sample was determined from standard curves generated using known concentrations of sodium nitrite.

Results are shown as the mean ± standard deviation of the data obtained in the five independent trials. Data were analysed using ANOVA followed by the Tukey multiple comparison test with GraphPad Prism 5 software ($p<0.05$).

2.7. Selection and description of immune related genes

Sequences from a public *P. lividus* ESTs database were automatically downloaded and reannotated (http://www.echinobase.org/Echinobase/,

http://goblet.molgen.mpg.de/cgi-bin/webapps/paracentrotus2008.cg) by using the Blast2GO software (Conesa et al., 2005). Cell mediated immune genes with a minimum eValue of 10e6 were searched. One sequence similar to a LPS-induced TNF-α factor (*Pl*-LITAF) (GenBank accession number KX083580) and two sequences similar to a macrophage migration inhibitory factor (*Pl*-MIFs and *Pl*-MIFl) (GenBank accession numbers KX083581 and KX083582) were selected. The sequences were translated using the ExPASy Proteomics Server tools and were compared with the sequences available in the GeneBank database using the BLAST tool and the ClustalW2 software. The compute pl/Mw program (Gasteiger et al., 2005) was used to determine their molecular weights and isoelectric points. The description of protein domains, families and functional sites was done using the PROSITE database and the Pfam software (Finn et al., 2010). Secondary structures were predicted according to the PSIPRED Server.

The phylogenetic analysis of the LITAF and MIF proteins was based on the entire *P. lividus* amino acid sequence, and 14 and 21 additional sequences of the LITAF and MIF family, respectively from vertebrates and invertebrates downloaded from the GenBank. As out-groups, a homologous LITAF sequence from *Streptococcus* spp. and a MIF sequence from plants were used. All sequences were aligned using MAFFT software (Katoh et al., 2005). Phylogenetic trees were constructed by the neighbor-joining method (Saitou and Nei, 1987) through MEGA software (Tamura et al., 2007). Nodal support was estimated using the same program with 10,000 bootstrap replicates.

2.8. Modulation of the *Pl*-LITAF and *Pl*-MIFs genes after PAMPs stimulation

Fifteen mL of CF were extracted from an animal, diluted 1:1 in ice-cold anti-clotting solution and dispensed into 24-well plates (BD). After 30 min at 15 °C in the

dark, the non-adherent cells were removed and the remaining cells were incubated at 15 ºC with 500 µl of solutions containing LPS, LTA, Poly I:C or Zymosan A (Sigma) at a final concentration of 100 µg/mL. Control animals were treated with FSW. After 3, 6 and 24 h, cells were washed twice with FSW and collected in 1 mL of Trizol reagent (Invitrogen). Adherent coelomocytes extracted from eight animals were used in the experiment.

Total RNA was extracted using Trizol reagent (Invitrogen) according to the manufacturer's protocol and treated with DNase I (Ambion). RNA (1 µg) was reverse transcribed into cDNA using SuperScript™ III Reverse Transcriptase (Invitrogen). Specific primers for qPCR were designed using the *Primer3* program (Rozen and Skaletsky, 2000) according to qPCR restrictions (Table 1). Dimer and hairpin formation was checked using the *Oligo Analyzer 1.0.2* software. The efficiency of each primer pair was analyzed with seven serial five-fold dilutions of cDNA, and the slope of the regression line of the quantification cycle versus the relative concentration of cDNA was calculated (Pfaffl, 2001). A melting curve analysis was also performed to verify that only specific amplification occurred. Real-Time PCR was performed with an Abi7300 Real Time PCR System (Applied Biosystems) using 1 µl cDNA with 12.5 µl SYBR green PCR master mix (Applied Biosystems) and 0.5 µl (10mM) of each specific primer. The relative expression levels of the genes were normalized using the ribosomal protein L17 (*Pl*-RPL17) gene as a reference gene (GeneBank accession number KX083583), which was constitutively expressed and not affected by the treatments, and analyzed following the Pfaffl method (Pfaffl, 2001). Results were expressed as the mean ± SD of the results obtained in the eight samples. Data were analysed using an ANOVA followed by the Tukey multiple comparison test ($p<0.05$).

3. Results and Discussion

3.1 Coelomocyte populations

Four main coelomocyte types were identified in *P. lividus*, the same result found by Gerardi et al., 1990; Pinsino et al., 2008; Deveci et al., 2015 in almost all sea urchin species. Petaloid cells (Figure 1, upper A) suffered a morphological transformation and developed multiple cytoplasmatic prolongations when spread on a glass substratum (Figure 1, right A). Two classes of spherule cells were easily differentiated, since they were either obviously red or colourless (Figure 1, middle A). The vibratile cells were propelled through the fluid by a single long flagellum (Figure 1, down A). The cell concentration in the CF of *P. lividus* ($2.4 \pm 0.35x10^6$ cells ml^{-1}) was similar to the one of other sea urchin species under healthy conditions (Bertheussen and Seljelid, 1978; Matranga et al., 2005). By flow cytometry, two main cell populations were distinguished (Figure 1, upper B), showing a FSC/SSC distribution similar to those of the starfish (*Asterias rubens*) (Coteur et al., 2002a) and the sea cucumber (*Apostichopus japonicus*) (Xing et al., 2008). The biggest and those who had more granules in their cytoplasm were included in the region 1 (R1) and represented a 63 % (± 5.4) of the total cell population. Cells included in the region 2 (R2) represented a 32 % (± 4.4) of the total cells. When coelomocytes were allowed to settle and spread and the non-adherent cells were removed, the number of cells in the R1 region increased up to 74 % (± 5.3) (Figure 1, down B). This result suggests the presence of amoeboid-phagocytes within the R1 region, since they are the only cell type with the ability to attach to surfaces (Ramírez-Gómez and García-Arrarás, 2010) and the presence of vibratile and spherule cells within the R2 region (Figure 1B).

3.2. Phagocytic activity and cell cooperation between coelomocytes

Phagocytosis plays an important role in the immunity of echinoderms (Smith et al., 2010). In echinoderms, phagocytosis has typically been analysed by optical microscopy, by counting the number of cells with phagocytic vesicles and the number of phagocytic vesicles per cell (Burke et al., 1991; Ito et al., 1992; Arizza et al., 2013). In the present work, flow cytometry technology has been applied to analyse the phagocytic activity in *P. lividus* as well as the cell cooperation between coelomocytes. To our knowledge, this is the first report describing the use of this technology in sea urchins.

The phagocytic activity of coelomocytes was registered as an increment in the FL1-H fluorescence levels, which is proportional to the number of ingested particles; the higher number of engulfed particles, the higher were the fluorescence levels (Figure 2A). The amoeboid-phagocytes included in the region R1 (the biggest and the most granulated cells) were the most active in the ingestion of particles (Figure 2B). A similar response was reported in starfish where the biggest and those who had more granules in their cytoplasm ingested the fluorescent bacteria (Coteur et al., 2002a; Xing et al., 2008). Phagocytic coelomocytes were able to ingest latex beads, *E. coli* and zymosan particles. Interestingly, cells ingested *E. coli* and zymosan particles preferentially over latex beads. Fifty percent (50%) of the cells engulfed Zymosan particles while less than 15% of the cells ingested latex beads (Figure 2C). Phagocytic coelomocytes were able to ingest up to 5 FITC-latex beads as observed by fluorescent microscopy (Figure 2C insert).

Cooperation between amoeboid-phagocytes and spherulocytes has been described in *P.lividus* resulting in an enhancement of the cytotoxic activity (Arizza et

al., 2007a). In order to explore if the cooperation between both cell types also affected the phagocytic activity, the phagocytic rates of samples that had been enriched in adherent cells (fractionated coelomocytes) were compared with those obtained using whole coelomocyte preparations (Figure 2D). The values of the phagocytosis obtained were significantly higher when we used whole coelomocyte populations than when we used fractionated samples (Figure 2D). A significant increase of zymosan and *E. coli* uptake (from 30 to 43 % and from 17 to 30 %, respectively) was observed. This result suggests that the cooperation between these two cellular types (amoeboid-phagocytes and spherulocytes) induces a higher phagocytic response. We could not rule out that the presence of compounds with opsonic activity in the coelomic fluid could be the cause of this increment of the phagocytic activity, as it was reported in the sea urchin *S. nodus* (Ito et al., 1992), in the sea star *A. forbesi* (Beck et al., 1993) and the sea cucumber *Holothuria leucospilota* (Xing and Chia, 2000).

3.3. Modulation of the phagocytic activity

The phagocytic process can be modulated by yeast and bacterial components such as glucans or CpGs, as it was reported in the sea cucumber *Apostichopus japonicus* (Gu et al., 2010; Li et al., 2009). In the *P. lividus*, gender differences in the phagocytic activity have been reported (Arizza et al., 2013). Also a decrease of this activity has been observed after an experimental cadmium exposure (Arizza et al., 2007b). In the present study, the treatment of coelomocytes from *P. lividus* with the different PAMPs induced significant changes in the relative percentage of phagocytic cells (Figure 3), reflecting the extremely complexity of the phagocytic process and the previous specific identification of non-self via specific TLR receptors (Russo et al., 2015).

Cells treated with LPS showed a significant increment in the uptake of latex beads and zymosan particles (Figure 3A), as it has been already described in LPS-stimulated coelomocytes from the sea cucumber *H. glaberrima* (Ramírez-Gómez et al., 2010). Interestingly LPS treatment also reduced the ingestion of *E. coli* particles. The treatment of cells with LTA increased the number of cells ingesting latex beads (Figure 3B) but also significantly reduced the phagocytosis of zymosan particles. Finally, Poly I:C treatment reduced the ingestion of latex beads (Figure 3C). The reduction of the phagocytic activity after stimulation suggests a possible competence for the surface receptors between the stimuli and the particles in agreement to the differential modulation of the *Pl-Tlr* gene after LPS or Poly I:C treatment (Russo et al., 2015).

3.4. Production of Reactive Oxygen Species (ROS) and Nitric Oxide (NO)

The production of reactive oxygen (ROS) is closely related to the phagocytic activity of coelomocytes in echinoderms (Coteur et al., 2002b, Sun et al., 2008). In holothurians, phagocytic coelomocytes produce ROS (Dolmatova et al., 2003) and in the sea urchin *P. lividus* the reactive oxygen species were mainly produced by cells included in the R1 region. An 82 % (± 5.7) of the FL-1 positive cells was located within this region (Figure 4A) suggesting that adherent amoeboid-phagocytes were the most active ROS producers in *P. lividus*. The soluble PMA did not affect the ROS production, similar to the response described in starfish and sea cucumber (Coteur et al., 2002b, 2005, Gu et al., 2010) (Figure 4B). The production of ROS was significantly increased in the presence of bacterial components. Cells treated with LPS and LTA showed a significant increase of ROS production, to double the production registered in the control group (Figure 4C and D). Interestingly, the stimulation with Zym and Poly

I:C induced a significant but lower production of ROS by coelomocytes (Figure 4E and 4F). Although the induction of ROS production by treatment with Poly I:C, a compound that mimics a viral infection, has been described in vertebrates (Yang et al., 2013), this response had not been previously reported in echinoderms.

Coelomocytes are also capable of producing and releasing NO upon stimulation with several microbial products (Beck et al., 2001; Romano et al., 2011). In our study, coelomocytes from the sea urchin *P. lividus* maintained a low basal level of NO (less than 5 μM), a situation previously described in starfish (Beck et al., 2001). Interestingly, the treatment of coelomocytes with PAMPs did not modify this production (data not shown), although similar treatments were able to increase the NO production in sea star and sea cucumber at 72 h post-treatment (Beck et al., 2001; Gu et al., 2010).

3.5. Selection and description of cell mediated immune response related genes

Since the publication of the genome of the sea urchin *S. purpuratus* (Sodergren et al., 2006) a lot of genomic and transcriptomic information has being generated from different echinoderm species and is available from public databases (http://www.echinobase.org/Echinobase/). Using the public *P. lividus* EST database (http://goblet.molgen.mpg.de/cgi-bin/webapps/paracentrotus2008.cgi) two cell mediated immune genes were selected and their regulation in coelomocytes was analyzed after PAMP stimulation. We selected a macrophage migration inhibitory factor (MIF) gene because it regulates the pro-inflammatory functions of immune cells in mammals during diseases, cell proliferation, tumor angiogenesis and development (Calandra and Roger, 2003; Javeed et al., 2008). Moreover, the novel transcription factor called LPS-induced TNF-α factor gene (LITAF) that regulates the expression of TNF-α and various

inflammatory cytokines in response to LPS in vertebrates (Myokai et al., 1999; Tang et al., 2005) was also selected.

3.5.1. Structural characterization of MIF and LITAF genes

MIF genes have been detected in most animals (mammals, birds, fish, amphibians, mollusks, nematodes, arthropods) and also in plants (Alexandrov et al., 2009; Buonocuore et al., 2010; Huang et al., 2016; Kim et al., 2010; Marson et al., 2001; Paralkar and Wistow, 1994; Suzuki et al., 2004; Wang et al., 2009). In echinoderms, the genome of the sea urchin *S. purpuratus* presented 9 MIF-like genes (Hibino et al., 2006). In the present work, the analysis of the public Pliv-EST database revealed the presence of at least two MIF genes in *P. lividus.* The first one called *Pl*-MIFlong was 417 bp long and encoded a 138-residues, non-glycosylated protein of 15.3 kDa. The second sequence called *Pl*-MIFshort was 348 bp long and encoded a 115 amino acid protein of 12.7 kDa. MIF genes in *P. lividus* showed similar structural features than those found in other vertebrates and invertebrates (Paralkar and Wistow, 1994; Wang et al., 2009). SMART software predicted the presence of MIF domains located between residues 2 and 114. The amino-terminal proline residue (P2) which is crucial for the catalytic activity, the site of isomerase activity (K33) and two out three sites of oxido-reductase activity (C57 and C60) are conserved in *Pl*-MIFs. The prediction of secondary structure showed two alpha-helices and five beta-sheets in the *Pl*-MIFs. (Supplementary figure 1A)

To date, the LITAF gene has been cloned in mollusks (De Zoysa et al., 2010), arthropods (Wang et al., 2012), fish (Wang et al., 2013), birds (Hong et al., 2006), and mammals (Myokai et al., 1999). In echinoderms only one partial EST with high identity to LITAF gene has been reported in *S. purpuratus* (Nair et al., 2005). The *Pl*-LITAF

sequence comprises an open reading frame (ORF) of 618 bp encoding a polypeptide of 205 amino acids with a theoretical isoelectric point of 5.85 and predicted molecular weight of 21.62 kDa. A characteristic LITAF domain located between residues 135 and 204, a N-terminal CXXC motif, followed by a long (25 residues) hydrophobic region and a C-terminal (H)XCXXC motif were identified, which is consistent with previous reports (Hong et al., 2006; Myokai et al., 1999; Wang et al., 2013). There were eight conserved Cys residues in the LITAF family domain that formed three canonical disulfide bridges (Supplementary figure 1B).

To examine the relationship of *Pl*-MIFs and *Pl*-LITAF genes with similar sequences in other species, several phylogenetic trees were constructed. The fact that the MIF genes were found in all the species studied, from plants to mammals suggests that the MIF genes are evolutionary conserved, most probably because of its functional significance. The branching pattern of *Pl*-MIFs and *Pl*-LITAF found corresponded essentially with the evolutionary relationship among the species (Supplementary Figure 2).

3.6. Modulation of the *Pl*-LITAF and *Pl*-MIFs genes after PAMPs stimulation

In order to gain a better understanding of the biological role of the *Pl*-MIFs and *Pl*-LITAF genes, we evaluated their expression levels in coelomocytes stimulated with PAMPs at different times post-stimulation (Figure 5).

The modulation of the MIF gene expression in echinoderms had never been analyzed before. *Pl*-MIFs genes (MIF-long and MIF-short) showed a similar behaviour after PAMPs stimulation (Figure 5A). Treatments with bacterial LPS and LTA did not induce any significant variation in the levels of gene expression. Interestingly, in other

invertebrates such as bivalve molluscs, the MIF gene was up-regulated in scallop hemocytes after lipopolysaccharide (LPS), peptidoglycan (PGN) and β-glucan stimulation (Li et al., 2011). Moreover, *in vivo* infection of the pearl oyster *Pinctada fucata* and the small abalone *Haliotis diversicolor* with *Vibrio alginolyticus* and *V. parahaemolyticus* (Cui et al., 2011; Wang et al., 2009) also induced the up-modulation of this gene. In the sea urchin *P. lividus* only zymosan and poly I:C treatments induced a significant increase of expression after 24 h reaching values up to 4 times over the controls (Figure 5A), suggesting that these two MIF genes could play a critical role in the inflammatory response to yeast or to viral infection.

The Pl-LITAF gene was up-regulated in coelomocytes treated with LPS at 6 and 24h. Up to an 8-fold increase in its expression over the controls (Figure 5B) was detected. A similar gene induction was previously reported by macroarray analysis in the sea urchin *S. purpuratus* 3 days after *in vivo* stimulation with LPS (Nair et al., 2005). Interestingly, although this gene is stimulated by LPS in the coelomocytes of *P. lividus*, a proteomic analysis of the coelomic fluid from *S. purpuratus* after stimulation with LPS was not able to detect this protein (Dheilly et al., 2013). The Gram-positive bacterial component LTA was not able to induce the expression of the LITAF gene (Figure 5B). A similar lack of response was described in other invertebrate models, such as in scallop hemocytes after treatment with peptidoglycan (Yu et al., 2007). The other non-bacterial PAMPs used (zymosan and Poly I:C) were capable of inducing LITAF expression (Figure 5B). This response has not been described before in echinoderms but it was described in the disk abalone (*Haliotis discus discus*) after viral infection (De Zoysa et al., 2010). These results could suggest that only the recognition of foreign particles by specific TLRs are able to initiate a signal transduction cascade leading to

TNF-a production through LITAF activation, as it was suggested in vertebrates (Hong et al., 2006; Tang et al., 2006).

In conclusion, we used the Mediterranean urchin *P. lividus* to explore some cellular immune mechanisms such as phagocytosis, cell cooperation, and ROS production using flow cytometry techniques. Moreover NO production and the induction of two cellular immune-related genes were evaluated after PAMP stimulation. Our results suggest that amoeboid-phagocytes are the most active immune cells involved in phagocytosis and ROS production. Moreover, the phagocytic response can be enhanced by cooperation between phagocytes and spherulocytes and is also modulated by PAMP stimulation. The coelomocytes are also activated by bacterial components as it is suggested by the high levels of expression of the MIF and LITAF genes detected by qPCR. Our results have helped us understand the cellular immune response mechanisms in the Mediterranean sea urchin *P. lividus* and their modulation after PAMP stimulation.

Acknowledgements

This work has been funded by the National Project A/026000/09 AECID, 2010-2012 “Respuesta inmune de invertebrados marinos”. We would like to thank Rubén Chamorro for his technical assistance in the aquarium.

Bibliography

Alexandrov, N.N., Brover, V.V., Freidin, S., Troukhan, M.E., Tatarinova, T.V., Zhang, H., Swaller, T.J., Lu, Y.P., Bouck, J., Flavell, R.B., Feldmann, K.A., 2009. Insights into corn genes derived from large-scale cDNA sequencing. Plant Mol. Biol. 69, 179-194.

Andrew, N.L., Agatsuma, Y., Ballesteros, E., Bazhin, A.G., Creaser, E.P., Barnes, D.K.A., Botsford, L.W., Bradbury, A., Campbell, A., Dixon, J.D., Einarsson, S., Gerring, P.K., Hebert, K., Hunter, M., Hur, S.B., Johnson, C.R., Juinio-Menez, M.A., Kalvass, P., Miller, R.J., Moreno, C.A., Palleiro, J.S., Rivas, D., Robinson, S.M.L., Schroeter, S.C., Steneck, R.S., Vadas, R.L., Woodby, D.A., Xiaoqi, Z., 2002. Status and management of world sea urchin fisheries. Oceanogr. Mar. Biol. 40, 343-425.

Arizza, V., Giaramita, F.T., Parrinello, D., Cammarata, M., Parrinello, N., 2007a. Cell cooperation in coelomocyte cytotoxic activity of *Paracentrotus lividus* coelomocytes. Comp. Biochem. Physiol. A. Mol. Integr. Physiol. 147, 389-394.

Arizza, V., Giaramita, F., Salerno, G., Vazzana, M., Basiricò, S., Parrinello, N., 2007b. Effect of cadmium exposure on phagocytosis and plaque lysis activity of *Paracentrotus lividus* coelomocyte. ISJ 4, 24-36.

Arizza, V., Vazzana, M., Schillaci, D., Russo, D., Giaramita, F.T., Parrinello, N., 2013. Gender differences in the immune system activities of sea urchin *Paracentrotus lividus*. Comp. Biochem. Physiol. A Mol. Integr. Physiol. 164, 447-455.

Beck, G., O'Brien, R.F., Habicht, G.S., Stillman, D.L., Cooper, E.L., Raftos, D.A., 1993. Invertebrate cytokines. III: Invertebrate interleukin-1-like molecules stimulate phagocytosis by tunicate and echinoderm cells. Cell Immunol. 146, 284-299.

Beck, G., Ellis, T., Zhang, H.Y., Lin, W.Y., Beauregard, K., Habicht, G.S., Truong, N., 2001. Nitric oxide production by coelomocytes of *Asterias forbesi*. Dev. Comp. Immunol. 25, 1-10.

Bertheussen, K., Seijelid, R., 1978. Echinoid phagocytes in vitro. Exp. Cell. Res. 111, 401-412.

Boudouresque, C.F., Verlaque, M., 2001. Ecology of *Paracentrotus lividus*, in: Miller Lawrence, J. (Ed.), Developments in Aquaculture and Fisheries Science. Edible Sea Urchins: Biology and Ecology 32, 177–216.

Brusca, R., Brusca, G., 2003. Invertebrates. Sunderland, Massachusetts: Sinauer Associates, Inc.

Buckley, K.M., Rast, J.P., 2012. Dynamic evolution of toll-like receptor multigene families in echinoderms. Front. Immunol. 3, 136.

Buonocore, F., Randelli, E., Facchiano, A.M., Pallavicini, A., Modonut, M., Scapigliati, G., 2010. Molecular and structural characterisation of a macrophage migration inhibitory factor from sea bass (*Dicentrarchus labrax* L.). Vet. Immunol. Immunopathol. 136, 297-304.

Burke, R.D., Watkins, R.F., 1991. Stimulation of starfish coelomocytes by interleukin-1. Biochem. Biophys. Res. Commun. 180, 5795-84.

Calandra, T., Roger, T., 2003. Macrophage migration inhibitory factor: a regulator of innate immunity. Nat. Rev. Immunol. 3, 791-800.

Canicattì, C., D'Ancona, G., 1989. Cellular aspects of *Holothuria polii* immune response. J. Invertebr. Pathol. 53, 152–158.

Chia, F.S., Xing, J., 1996. Echinoderm Coelomocytes. Zool. Stud. 35, 231-254.

Conesa, A., Götz, S., García-Gómez, J.M., Terol, J., Talón, M., Robles, M., 2005. Blast2GO: A universal tool for annotation, visualization and analysis in functional genomics research. Bioinformatics 21, 3674-3676.

Coteur, G., DeBecker, G., Warnau, M., Jangoux, M., Dubois, P., 2002a. Differentiation of immune cells challenged by bacteria in the common European starfish, *Asterias rubens* (Echinodermata). Eur. J. Cell. Biol. 81, 413-418.

Coteur, G., Warnau, M., Jangoux, M., Dubois, P., 2002b. Reactive oxygen species (ROS) production by amoebocytes of *Asterias rubens* (Echinodermata). Fish Shellfish Immunol. 12, 187-200.

Coteur, G., Danis, B., Dubois, P., 2005. Echinoderm reactive oxygen species (ROS) production measured by peroxidase, luminol-enhanced chemiluminescence (PLCL) as an immunotoxicological tool. Prog. Mol. Subcell. Biol. 39, 71-83.

Cui, S., Zhang, D., Jiang, S., Pu, H., Hu, Y., Guo, H., Chen, M., Su, T., Zhu, C., 2011. A macrophage migration inhibitory factor like oxidoreductase from pearl oyster *Pinctada fucata* involved in innate immune responses. Fish Shellfish Immunol. 31, 173-181.

Deveci, R., Şener, E., İzzetoğlu, S., 2015. Morphological and ultrastructural characterization of sea urchin immune cells. J Morphol. doi: 10.1002/jmor.20368.

De Zoysa, M., Nikapitiya, C., Oh, C., Whang, I., Lee, J.S., Jung, S.J., Choi, C.Y., Lee, J., 2010. Molecular evidence for the existence of lipopolysaccharide-induced TNF-alpha factor (LITAF) and Rel/NF-kB pathways in disk abalone (*Haliotis discus discus*). Fish Shellfish Immunol. 28, 754e63.

Dheilly, N.M., Haynes, P.A., Bove, U., Nair, S.V., Raftos, D.A., 2011. Comparative proteomic analysis of a sea urchin (*Heliocidaris erythrogramma*) antibacterial response revealed the involvement of apextrin and calreticulin. J. Invertebr. Pathol. 106, 223-229.

Dheilly, N.M., Raftos, D.A., Haynes, P.A., Smith, L.C., Nair, S.V., 2013. Shotgun proteomics of coelomic fluid from the purple sea urchin, *Strongylocentrotus purpuratus*. Dev. Comp. Immunol. 40, 35-50.

Dheilly, N.M., Haynes, P.A., Raftos, D.A., Nair, S.V., 2012. Time course proteomic profiling of cellular responses to immunological challenge in the sea urchin, *Heliocidaris erythrogramma*. Dev. Comp. Immunol. 37, 243-256.

Dolmatova, L.S., Eliseykina, M.G., Timchenko, N.F., Kovaleva, A.L., Shitkova, O.A., 2003. Generation of reactive oxygen species in different fractions of the coelomocytes of Holothurian *Eupentacta fraudatrix* in response to the thermostable toxin of *Yersinia pseudotuberculosis* in vitro. Chin. J. Oceanol. Limnol. 24, 293-304.

Du, J., Xie, X., Chen, H., Yang, W., Dong, M., Su, J., Wang, Y., Yu, C., Zhang, S., Xu, A., 2004. Macrophage migration inhibitory factor (MIF) in chinese amphioxus as a molecular marker of immune evolution during the transition of invertebrate/vertebrate. Dev. Comp. Immunol. 28, 961-971.

Edds, K.T., 1993. Cell biology of echinoid coelomocytes I. Diversity and characterization of cell types. J. Invertebr. Pathol. 61, 173-178.

Finn, R.D., Mistry, J., Tate, J., Coggill, P., Heger, A., Pollington, J.E., Gavin, O.L., Gunasekaran, P., Ceric, G., Forslund, K., Holm, L., Sonnhammer, E.L., Eddy,

S.R., Bateman, A., 2010. The Pfam protein families database. Nucleic Acids Res. 38, D211-222.

Gasteiger, E., Hoogland, C., Gattiker, A., Duvaud, S., Wilkins, M.R., Appel, R.D., Bairoch, A., 2005. Protein Identification and Analysis Tools on the ExPASy Server in: Walker, J.M. (Eds.), The Proteomics Protocols Handbook. Humana Press Inc., Totowa, NJ.

Gerardi, G., Lassegues, M., Canicattì, C., 1990. Cellular distribution of sea urchin antibacterial activity. Biol. Cell 120, 161–165.

Green, L.C., Wagner, D.A., Glogowski, J., Skipper, P.L., Wishnok, J.S., Tannenbaum, S., 1982. Analysis of nitrate, nitrite and (15N) nitrate in biological fluids. Anal. Biochem. 126, 131-138.

Gross, P.S., Al-Sharif, W.Z., Clow, L.A., Smith, L.C., 1999. Echinoderm immunity and the evolution of the complement system. Dev. Comp. Immunol. 23, 429-442.

Gu, M., Ma, H., Mai, K., Zhang, W., Ai, Q., Wang, X., Bai, N., 2010. Immune response of sea cucumber *Apostichopus japonicus* coelomocytes to several immunostimulants in vitro. Aquaculture 306, 49–56.

Guidetti, P., Dulcić, J., 2007. Relationships among predatory fish, sea urchins and barrens in Mediterranean rocky reefs across a latitudinal gradient. Mar. Environ. Res. 63, 168-184.

Haug, T., Kjuul, A.K., Styrvold, O.B., Sandsdalen, E., Olsen, O.M., Stensvag, K., 2002. Antibacterial activity in *Strongylocentrotus droebachiensis* (Echinoidea), *Cucumaria frondosa* (Holothuroidea), and *Asterias rubens* (Asteroidea). J. Invertebr. Pathol. 81, 94–102.

Hereu, B., Zabala, M., Linares, C., Sala, E., 2005. The effects predator abundance and habitat structural complexity on survival juvenile sea urchins. Mar. Biol. 146, 293–299.

Hibino, T., Loza-Coll, M., Messier, C., Majeske, A.J., Cohen, A.H., Terwilliger, D.P., Buckley, K.M., Brockton, V., Nair, S.V., Berney, K., Fugmann, S.D., Anderson, M.K., Pancer, Z., Cameron, R.A., Smith, L.C., Rast, J.P., 2006. The immune gene repertoire encoded in the purple sea urchin genome. Dev. Biol. 300, 349-65.

Hong, Y.H., Lillehoj, H.S., Lee, S.H., Park, D.W., Lillehoj, E.P., 2006. Molecular cloning and characterization of chicken lipopolysaccharide-induced TNF-alpha factor (LITAF). Dev. Comp. Immunol. 30, 919-929.

Huang WS, Duan LP, Huang B, Wang KJ, Zhang CL, Jia QQ, Nie P, Wang T., 2016. Macrophage migration inhibitory factor (MIF) family in arthropods: cloning and expression analysis of two MIF and one D-dopachrome tautomerase (DDT) homologues in Mud crabs, *Scylla paramamosain*. Fish Shellfish Immunol. S1050-4648 (16), 30030-4.

Inohara, N., Chamaillard, M., McDonald, C., Nunez, G., 2005. NOD-LRR proteins: role in host-microbial interactions and inflammatory disease. Annu. Rev. Biochem. 74, 355-383.

Ito, T., Matsutani, T., Mori, K., Nomura, T., 1992. Phagocytosis and hydrogen peroxide production by phagocytes of the sea urchin *Strongylocentrotus nudus*. Dev. Comp. Immunol. 16, 287-294.

Javeed, A., Zhao, Y., Zhao, Y., 2008. Macrophage-migration inhibitory factor: role in inflammatory diseases and graft rejection. Inflamm. Res. 57, 45-50.

Jin, P., Hu, J., Qian, J., Chen, L., Xu, X., Ma, F., 2012. Identification and characterization of a putative lipopolysaccharide-induced TNF-α factor (LITAF) gene from Amphioxus (*Branchiostoma belcheri*): an insight into the innate immunity of Amphioxus and the evolution of LITAF. Fish Shellfish Immunol. 32, 1223-1228.

Katoh, K., Kuma, K., Toh, H., Miyata, T., 2005. MAFFT version 5: improvement in accuracy of multiple sequence alignment. Nucleic Acids Res. 33, 511-518.

Kim, S., Miska, K.B., Jenkins, M.C., Fetterer, R.H., Cox, C.M., Stuard, L.H., Dalloul, R.A., 2010. Molecular cloning and functional characterization of the avian macrophage migration inhibitory factor (MIF). Dev. Comp. Immunol. 34, 1021-1032.

Kondo, M., Akasaka, K., 2012. Current Status of Echinoderm Genome Analysis - What do we Know? Curr. Genomics. 13, 134-143.

Li, F.M., Huang, S.Y., Wang, L.L., Yang, J.L., Zhang, H., Qiu, L.M., Li, L., Song, L.A., 2011. A macrophage migration inhibitory factor like gene from scallop *Chlamys farreri*: involvement in immune response and wound healing. Dev. Comp. Immunol. 35, 62e71.

Li, J., Sun, X., Zheng, F., Hao, L., 2009. Screen and effect analysis of immunostimulants for sea cucumber, *Apostichopus japonicus*. Chin. J. Oceanol. Limnol. 27, 80-84.

Lin, W., Zhang, H., Beck, G., 2001. Phylogeny of natural cytotoxicity: cytotoxic activity of coelomocytes of the purple sea urchin, *Arbacia punctulata*. J. Exp. Zool. 290, 741–750.

Marson, A.L., Tarr, D.E., Scott, A.L., 2001. Macrophage migration inhibitory factor (MIF) transcription is significantly elevated in *Caenorhabditis elegans* dauer larvae. Gene. 278, 53-62.

Matranga, V., 1996. Molecular Aspects of Immune Reactions in Echinodermata. Invertebrate Immunology. Prog. Mol. Subcell. Biol. 15, 235-247.

Matranga, V., Pinsino, A., Celi, M., Natoli, A., Bonaventura, R., Schröder, H.C., et al., 2005. Monitoring chemical and physical stress using sea urchin immune cells. Prog. Mol. Subcell. Biol. 39, 85–110.

Matranga, V., Toia, G., Bonaventura, R., Müller, W.E., 2000. Cellular and biochemical responses to environmental and experimentally induced stress in sea urchin coelomocytes. Cell Stress Chaperon. 5, 113-120.

Metchnikoff, I., 1891. Lectures on the comparative pathology of inflammation. Delivered at the Pasteur Institute in 1891. New York.

Myokai, F., Takashiba, S., Lebo, R., Amar, S., 1999. A novel lipopolysaccharide-induced transcription factor regulating tumor necrosis factor alpha gene expression: molecular cloning, sequencing, characterization, and chromosomal assignment. Proc. Natl. Acad. Sci. U S A 96, 4518-23.

Nair, S.V., Del Valle, H., Gross, P.S., Terwilliger, D.P., Smith, L.C., 2005. Macroarray analysis of coelomocyte gene expression in response to LPS in the sea urchin. Identification of unexpected immune diversity in an invertebrate. Physiol. Genomics 22, 33-47.

Pancer, Z., 2000. Dynamic expression of multiple scavenger receptor cysteine-rich genes in coelomocytes of the purple sea urchin. Proc. Natl. Acad. Sci. U S A 97, 13156-13161.

Paralkar, V., Wistow, G., 1994. Cloning the human gene for macrophage migration inhibitory factor (MIF). Genomics 19, 48-51.

Pfaffl, M.W., 2001. A new mathematical model for relative quantification in real-time RT-PCR. Nucleic Acids 29, e45.

Pinsino, A., Thorndyke, M.C., Matranga, V., 2007. Coelomocytes and post-traumatic response in the common sea star *Asterias rubens*. Cell Stress Chaperon. 12, 331-341.

Pinsino, A., Della Torre, C., Sammarini, V., Bonaventura, R., Amato, E., Matranga, V., 2008. Sea urchin coelomocytes as a novel cellular biosensor of environmental stress: a field study in the Tremiti Island Marine Protected Area, Southern Adriatic Sea, Italy. Cell Biol. Toxicol. 24, 541-552.

Ramírez-Gómez, F., Aponte-Rivera, F., Méndez-Castaner, L., García-Arrarás, J.E., 2010. Changes in holothurian coelomocyte populations following immune stimulation with different molecular patterns. Fish Shellfish Immunol. 29, 175-185.

Ramírez-Gómez, F., García-Arrarás, J.E., 2010. Echinoderm immunity. ISJ 7, 211-220.

Rast, J.P., Pancer, Z., Davidson, E.H., 2000. New approaches towards an understanding of deuterostome immunity. Curr. Top. Microbiol. Immunol. 248, 3-16.

Rast, J.P., Smith, L.C., Loza-Coll, M., Hibino, T., Litman, G.W., 2006. Genomic insights into the immune system of the sea urchin. Science 314, 952-956.

Romano, G., Costantini, M., Buttino, I., Ianora, A., Palumbo, A., 2011. Nitric oxide mediates the stress response induced by diatom aldehydes in the sea urchin *Paracentrotus lividus*. PLoS One 6, e25980

Rozen, S., Skaletsky, H.J., 2000. Primer3 on the WWW for general users and for biologist programmers. Methods Mol. Biol. 132, 365-386.

Russo, R., Chiaramonte, M., Matranga, V., Arizza, V., 2015. A member of the TLR family is involved in the innate immune response to dsRNA *Paracentrotus lividus* sea urchin. Dev. Comp. Immunol. 51, 271-277.

Saitou, N., Nei, M., 1987. The neighbor-joining method: a new method for reconstructing phylogenetic trees. Mol. Biol. Evol. 4, 406-425.

Smith, L.C., 2010. Diversification of innate immune genes: lessons from the purple sea urchin. Dis. Model. Mech. 3, 274-279.

Smith, L.C., Ghosh, J., Buckley, K.M., Clow, L.A., Dheilly, N.M., Haug, T., Henson, J.H., Li, C., Lun, C.M., Majeske, A.J., Matranga, V., Nair, S.V., Rast, J.P., Raftos, D.A., Roth, M., Sacchi, S., Schrankel, C.S., Stensvåg, K., 2010. Echinoderm immunity. Adv. Exp. Med. Biol. 708, 260-301.

Sodergren, E., Weinstock, G.M., Davidson, E.H., Cameron, R.A., Gibbs, R.A., Angerer, R.C., et al., 2006. The genome of the sea urchin *Strongylocentrotus purpuratus*. Science 314, 941-952.

Sun, Y., Jin, L., Wang, T., Xue, J., Liu, G., Li, X., You, J., Li, S., Xu, Y., 2008. Polysaccharides from *Astragalus membranaceus* promote phagocytosis and superoxide anion (O2-) production by coelomocytes from sea cucumber *Apostichopus japonicus* in vitro. Comp. Biochem. Physiol. C Toxicol. Pharmacol. 147, 293-298.

Suzuki, M., Takamura, Y., Maeno, M., Tochinai, S., Iyaguchi, D., Tanaka, I., Nishihira, J., Ishibashi, T., 2004. *Xenopus laevis* macrophage migration inhibitory factor is essential for axis formation and neural development. J. Biol. Chem. 279, 21406–21414.

Tamura, K., Dudley, J., Nei, M., Kumar, S., 2007. MEGA4: Molecular Evolutionary Genetics Analysis (MEGA) software version 4.0. Mol. Biol. Evol. 24, 1596-1599.

Tang, X., Metzger, D., Leeman, S., Amar, S., 2006. LPS-induced TNF-alpha factor (LITAF)-deficient mice express reduced LPS-induced cytokine: Evidence for LITAF dependent LPS signaling pathways. Proc. Natl. Acad. Sci. U S A 103, 13777-81372.

Tang, X., Marciano, D.L., Leeman, S.E., Amar, S., 2005. LPS induces the interaction of a transcription factor, LPS-induced TNF-afactor, and STAT6(B) with effects on multiple cytokines. Proc. Natl. Acad. Sci. USA 102, 5132. e7.

Terwilliger, D.P., Buckley, K.M., Brockton, V., Ritter, N.J., Smith, L.C., 2007. Distinctive expression patterns of 185/333 genes in the purple sea urchin, *Strongylocentrotus purpuratus*: an unexpectedly diverse family of transcripts in response to LPS, beta-1,3-glucan, and dsRNA. BMC Mol. Biol. 8, 16.

Wang, P.H., Wan, D.H., Pang, L.R., Gu, Z.H., Qiu, W., Weng, S.P., Yu, X.Q., He, J.G., 2012. Molecular cloning, characterization and expression analysis of the tumor necrosis factor (TNF) superfamily gene, TNF receptor superfamily gene and lipopolysaccharideinduced TNF-alpha factor (LITAF) gene from *Litopenaeus vannamei*. Dev. Comp. Immunol. 36, 39e50.

Wang, H., Shen, X., Xu, D., Lu, L., 2013. Lipopolysaccharide-induced TNF-α factor in grass carp (*Ctenopharyngodon idella*): evidence for its involvement in antiviral innate immunity. Fish Shellfish Immunol. 34, 538-545.

Wang, B., Zhang, Z., Wang, Y., Zou, Z., Wang, G., Wang, S., Jia, X., Lin, P., 2009. Molecular cloning and characterization of macrophage migration inhibitory factor from small abalone *Haliotis diversicolor* supertexta. Fish Shellfish Immunol. 27, 57-64.

Xing, K., Yang, H.S., Chen, M.Y., 2008. Morphological and ultrastructural characterization of the coelomocytes in *Apostichopus japonicus*. Aquat. Biol. 2, 85-92.

Xing, J., Chia, F.S., 2000. Opsonin-like molecule found in coelomic fluid of a sea cucumber, *Holothuria leucospilota*. Mar. Biol. 136, 979-986.

Yang, C.S., Kim, J.J., Lee, S.J., Hwang, J.H., Lee, C.H., Lee, M.S., Jo, E.K., 2013. TLR3-Triggered Reactive Oxygen Species Contribute to Inflammatory Responses by Activating Signal Transducer and Activator of Transcription-1. J. Immunol. 190, 6368-6377.

Yu, Y., Qiu, L., Song, L., Zhao, J., Ni, D., Zhang, Y., Xu, W., 2007. Molecular cloning and characterization of a putative lipopolysaccharide-induced TNF-alpha factor

(LITAF) gene homologue from Zhikong scallop *Chlamys farreri*. Fish Shellfish Immunol. 23, 419-429.

Figure legends.

Figure 1: (A) Coelomocytes of the sea urchin *Paracentrotus lividus*. Petaloid amoebocyte (Upper A). Spread amebocyte with cytoplasmatic prolongations (Right A). Red and colourless spherule cells (Middle A). Vibratile cell (Down A). Scale bar 10 µm. **(B) Separation of coelomocytes by forward and sideward scatter (FSC/SSC) flow cytometry.** Density plots of CF samples diluted 1:1 in anti-clotting solution immediately after the extraction (Upper B). Density plots of samples enriched in adherent cells (Down B). 150,000 events were represented.

Figure 2: Evaluation of the phagocytic activity by flow cytometry. (A) Histogram showing the fluorescence levels (FL1-H) registered in cells after ingestion of FITC-labelled particles. **(B)** The phagocytic cells were mainly included in the region R1. **(C)** Percentage of cells ingesting zymosan, *E. coli* and latex beads. Example of amoebocyte engulfing different number of fluorescence latex beads after a 2 h incubation. Scale bar 25 µm. **(D)** Percentage of phagocitosis (mean ± standard deviation) using samples containing all coelomocyte populations (whole coelomocytes) or samples enriched in adherent cells (Fractionated coelomocytes). Data were analysed using Student's t-test and differences were statistically significant at $p<0.05$. (*) Significant differences compared to the results obtained using fractionated coelomocyte samples.

Figure 3: Percentage of phagocytic cells engulfing different FITC-particles (latex beads, *E. coli* or zymosan) after 2 h of stimulation with 25 or 50 µg/mL of LPS (A), LTA (B) and poly I:C (C). Each bar represents the mean and standard error of six biological replicates. (*) Significant differences compared to the non-stimulated control group ($p<0.05$).

Figure 4: (A) Location of cells producing ROS within the overall cell population by flow cytometry. Measurement of ROS production after stimulation with PMA (B) LPS (C), LTA (D), Zymosan A (E) or Poly I:C (F) (25 and 50 µg/mL). Each bar represents the mean and standard error of six biological replicates. (*) Significant differences compared to the control group ($p<0.05$).

Figure 5: Changes in the expression of *Pl*-MIFs (A) and *Pl*-LITAF (B) genes after stimulation with LPS, LTA, Zymosan and Poly I:C. The RPL17 gene was used as the housekeeping control gene. Data represents the mean ± SD of eight individual samples, each assayed performed in triplicate. (*) Significant differences compared to the level of expression level obtained 3 h post-stimulation ($p\leq0.05$).

Supplementary figure 1: (A) Multiple alignment of the MIF amino acid sequences from 13 different species. Important residues for catalytic activity, isomerase activity and oxido-reductase activity are black boxed. Residues believed to be involved in the tautomerase activity are highlighted in gray. The positions of alpha-helices and beta-sheets are indicated. **(B)** Amino acid alignment of Pl-LITAF with known LITAF sequences. Identical amino acids are highlighted by black boxes and asterisks (*).The predicted LITAF domain, which contains two CXXC motifs, is indicated above the sequence.

Supplementary figure 2: Phylogenetic relationships of the MIF **(A)** and LITAF **(B)** proteins from different species. The trees were constructed using the Neighbour-Joining algorithm within MEGA (version 3.0). The degree of confidence for each branch point was determined by bootstrap analysis (10,000 repetitions).

Table 1: Sequences of primers for Real-Time PCR.

Name	Sequence	Ct slope	Contig Nº	GenBank Nº
LITAF 1F	CGGATTGTGGTTCTTTTGCT	-3.23	7190	
LITAF 1R	CACAGGGCATGTATGGACAG			
MIFs 1F	AAGCAATTGGGAAACCACAG	-3.34	11052	
MIFs 1R	GTTGATCCCGCAAAACTCAT			
MIFl 1F	GCTCGCAGTATTTGTCACGA	-3.40	10606	
MIFl 1R	CGATGGAGTCTGTCGCATAA			
RPL17 1F	GGCTCCTACCTTCGTGTTCA	-3.31	7395	
RPL17 1R	GCATGTGCTTGATAGCCTGA			

Figure 1

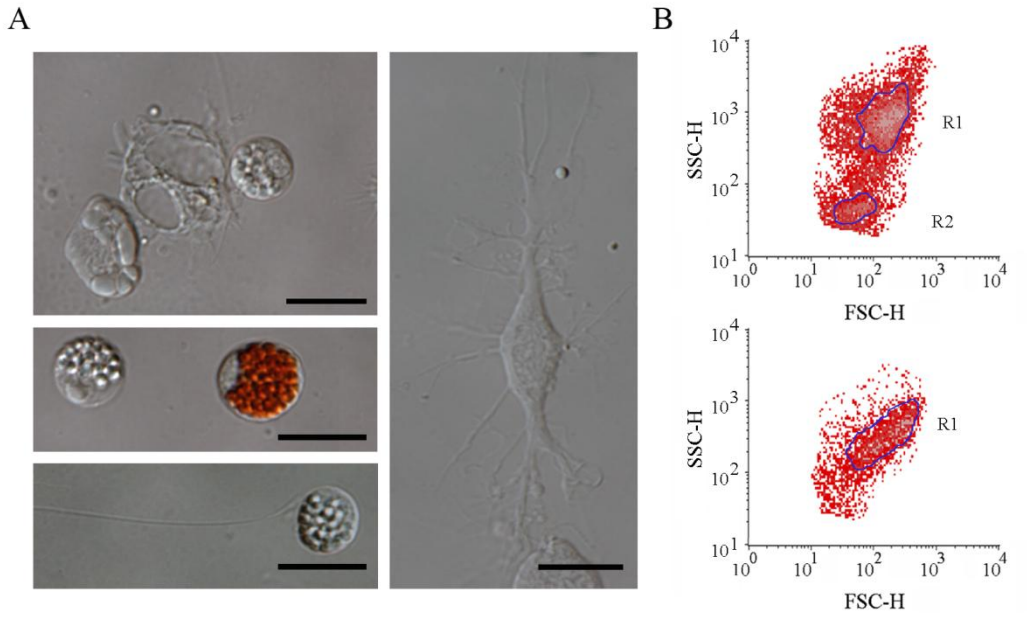

Figure 2

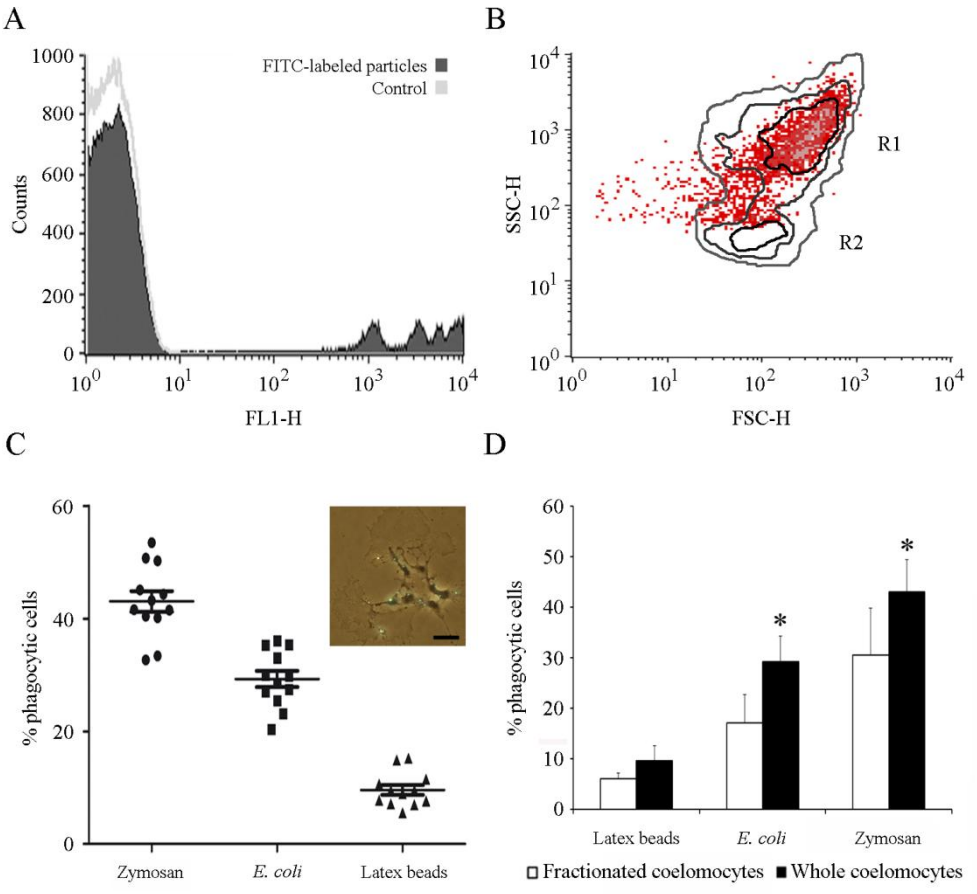
A
FITC-labeled particles
Control
Counts
FL1-H
B
SSC-H
FSC-H
R1
R2
C
% phagocytic cells
Zymosan
E. coli
Latex beads
D
% phagocytic cells
Latex beads
E. coli
Zymosan
Fractionated coelomocytes
Whole coelomocytes

Figure 3

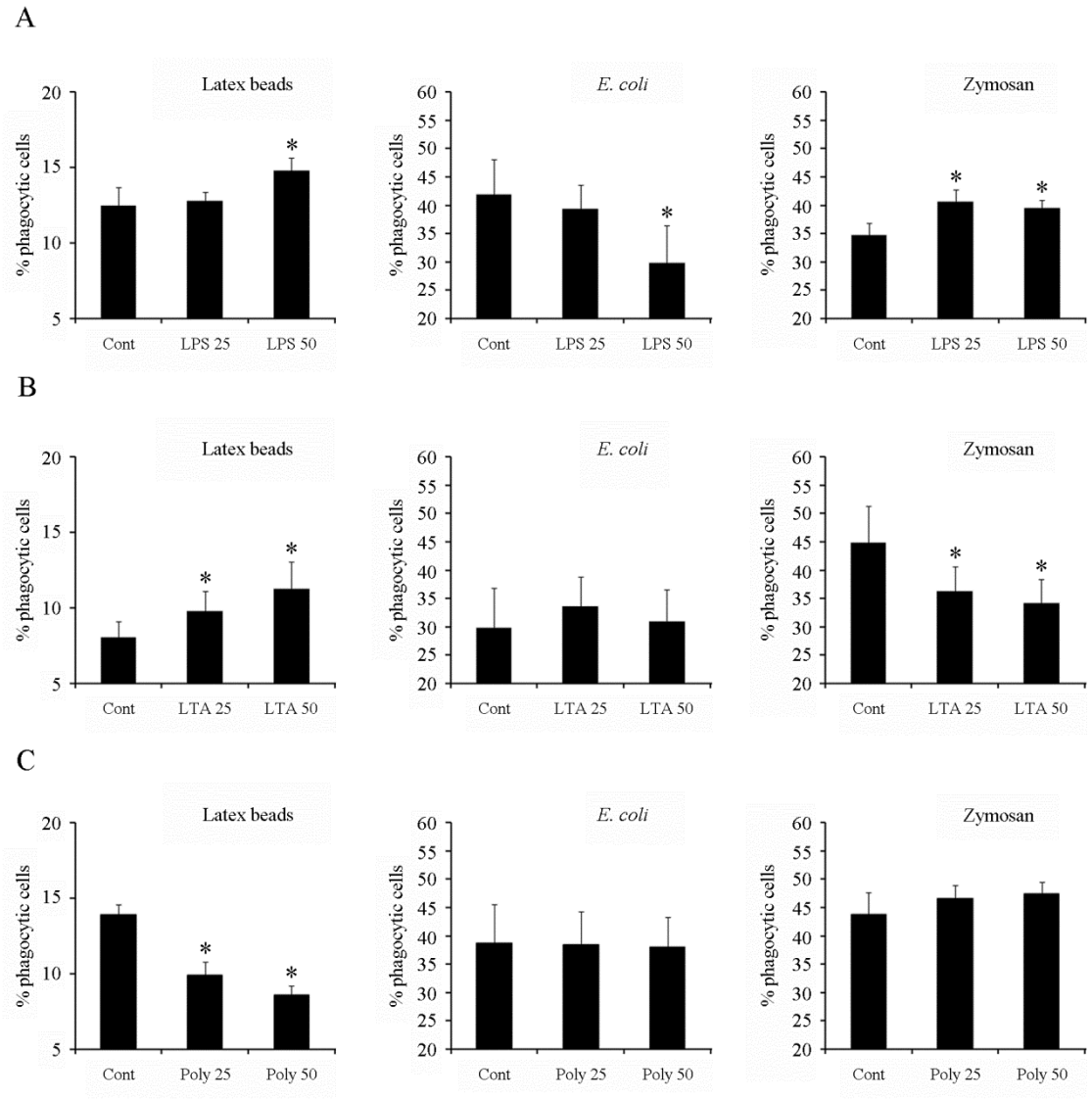
A
Latex beads
E. coli
Zymosan
% phagocytic cells
Cont
LPS 25
LPS 50
B
Latex beads
E. coli
Zymosan
% phagocytic cells
Cont
LTA 25
LTA 50
C
Latex beads
E. coli
Zymosan
% phagocytic cells
Cont
Poly 25
Poly 50

Figure 4

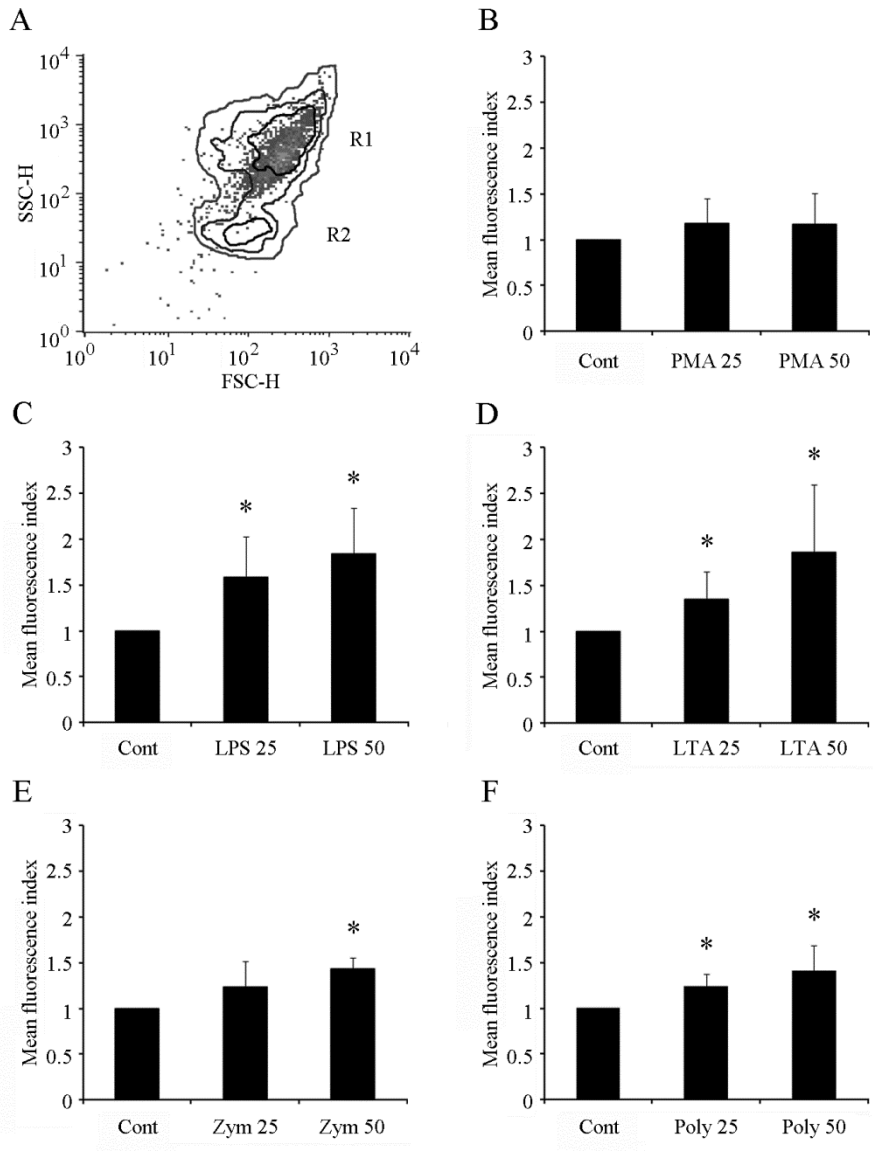
A
B
C
D
E
F
SSC-H
FSC-H
R1
R2
Mean fluorescence index
Cont
PMA 25
PMA 50
LPS 25
LPS 50
LTA 25
LTA 50
Zym 25
Zym 50
Poly 25
Poly 50

Figure 5

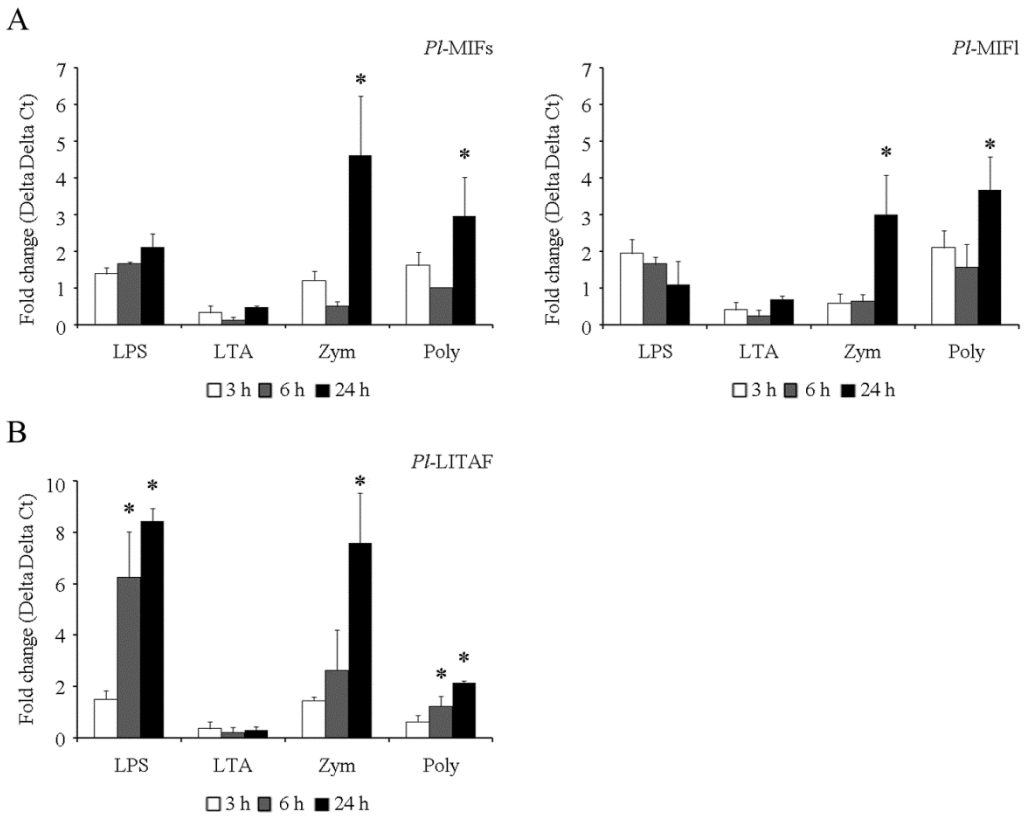
A
Pl-MIFs
Fold change (Delta Delta Ct)
LPS
LTA
Zym
Poly
3 h
6 h
24 h
Pl-MIF1
B
Pl-LITAF

Supplementary figure 1

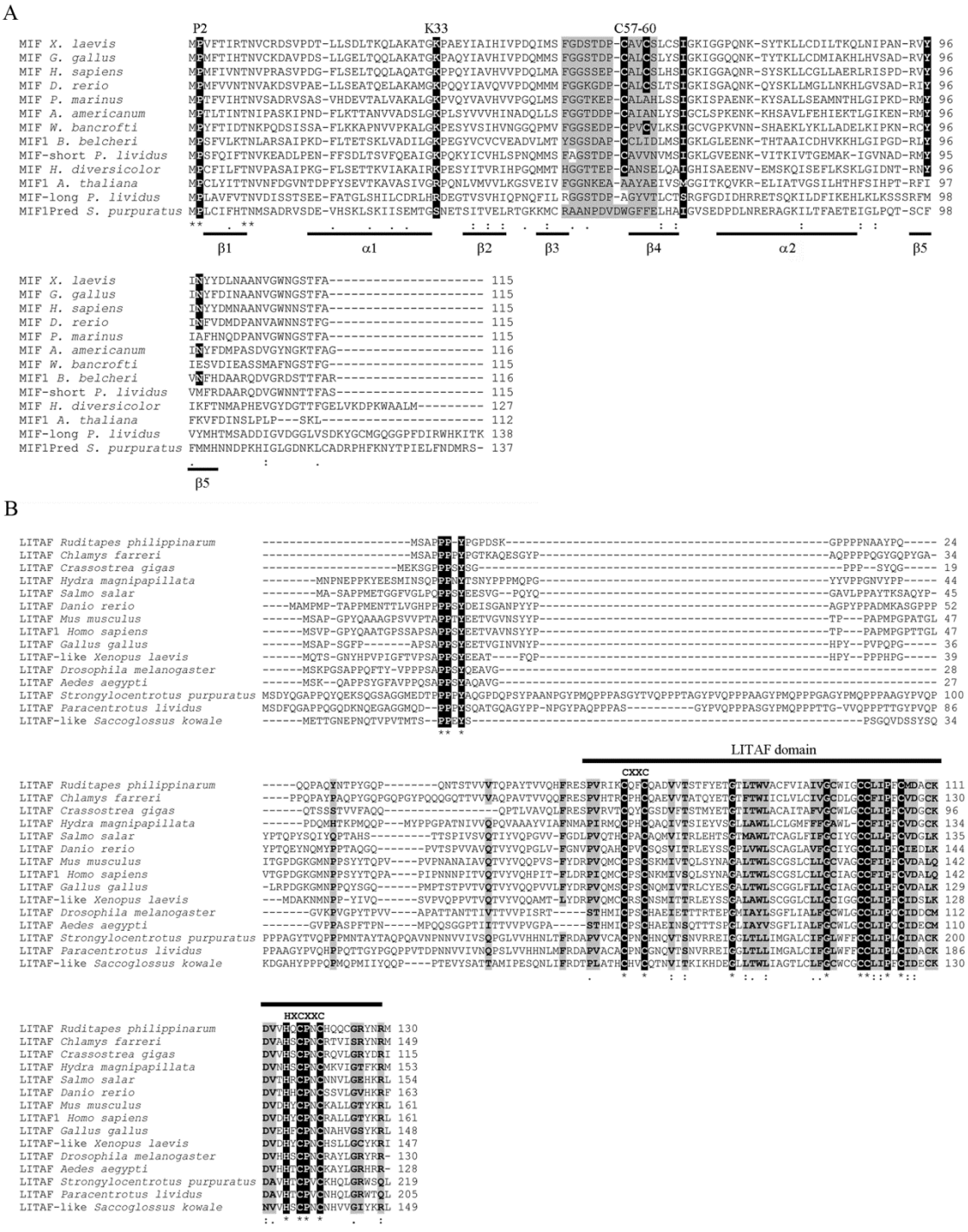

Supplementary figure 2

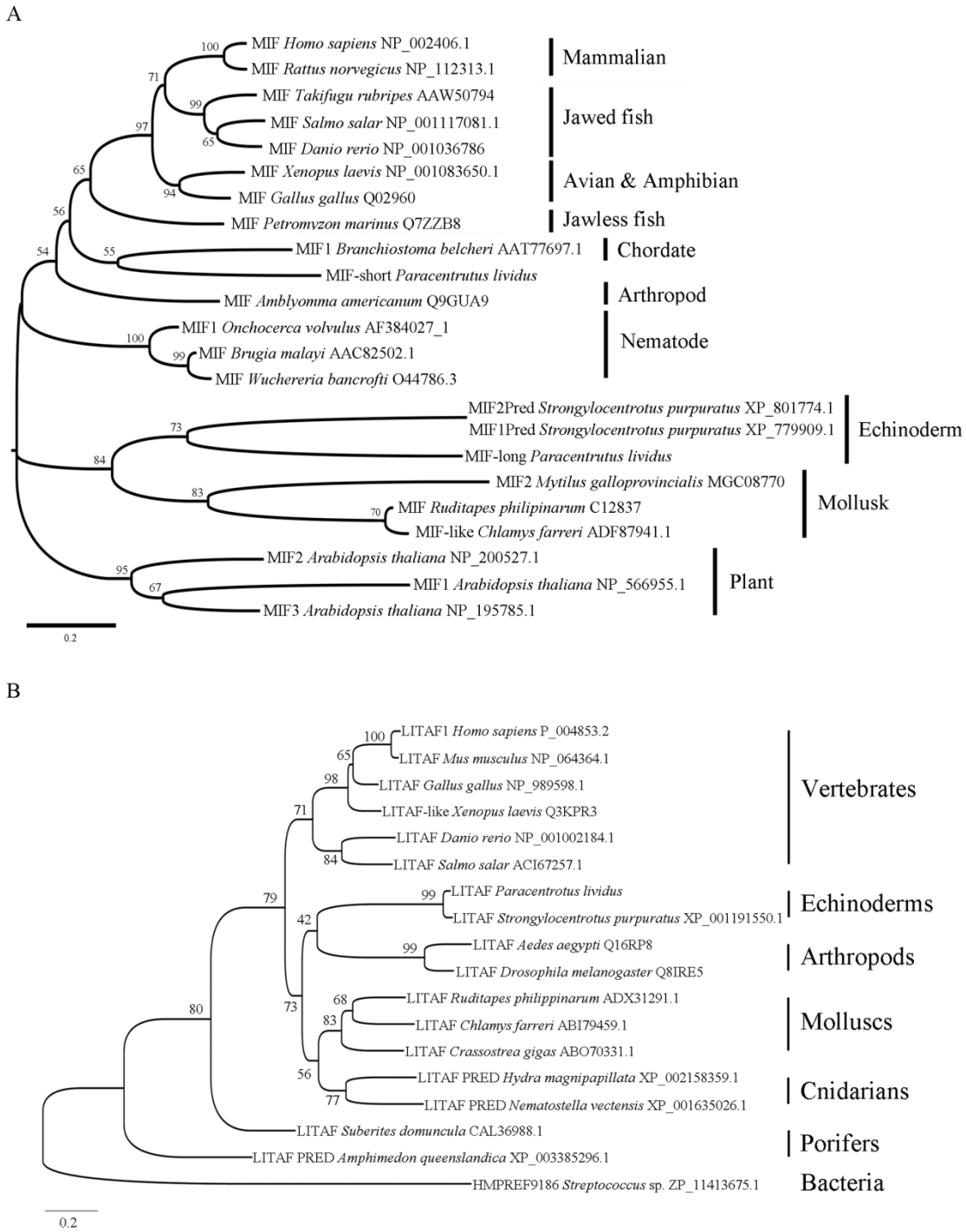

Figure 1

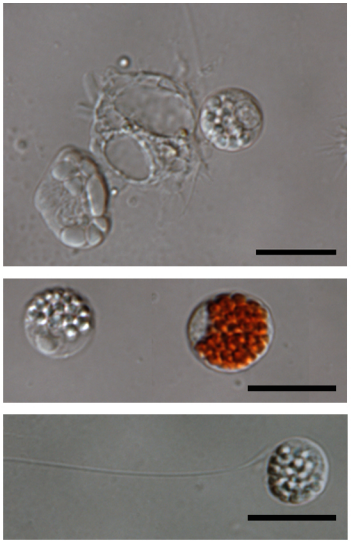

B

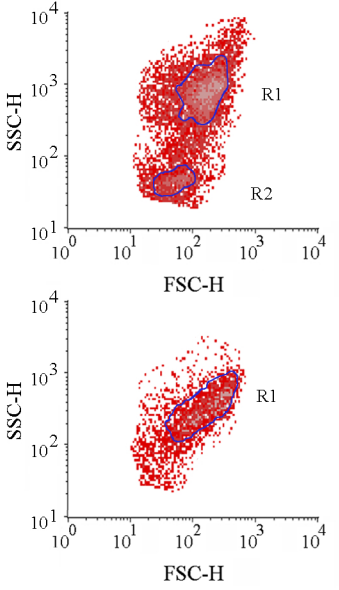

Figure 2

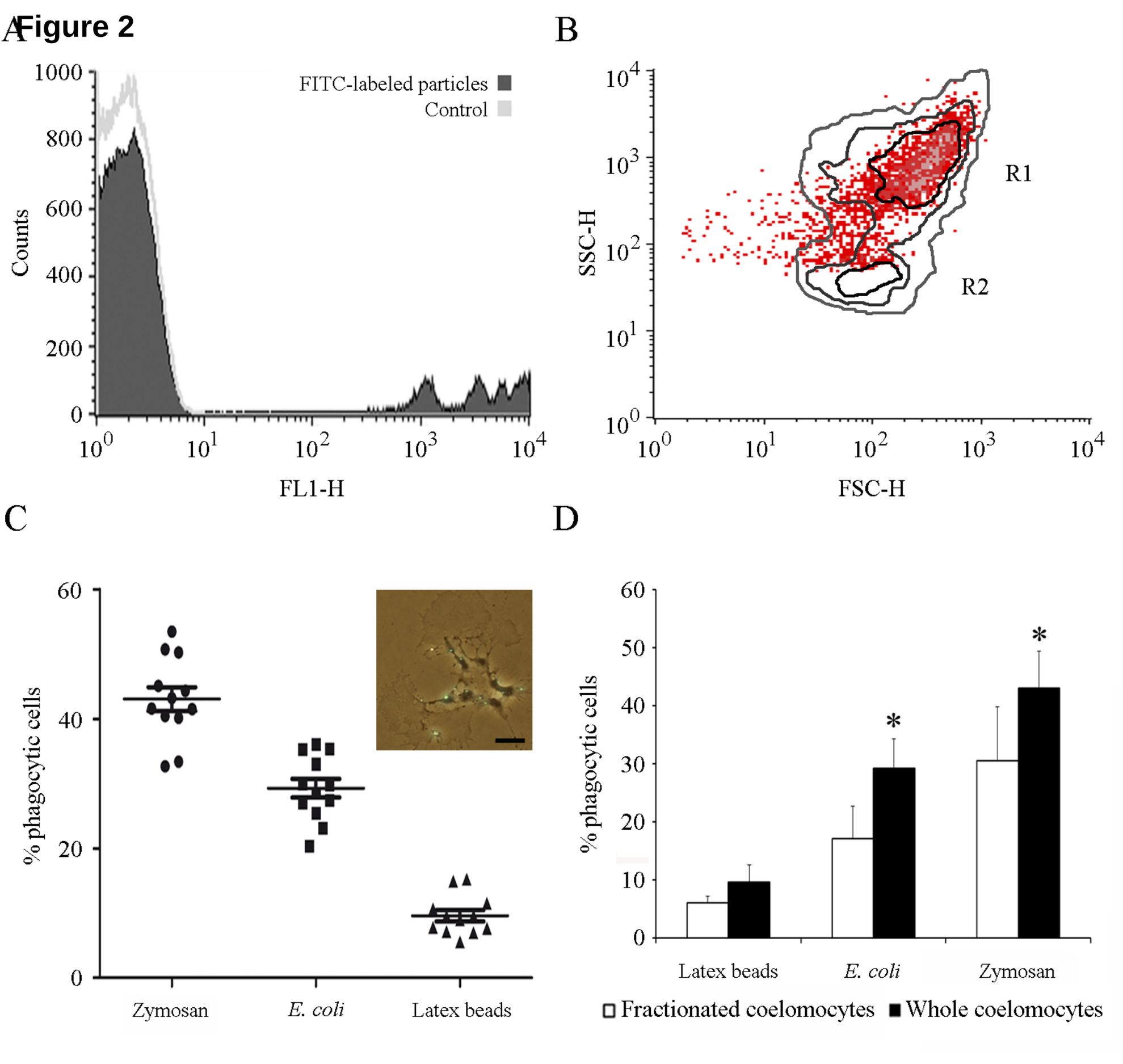
A
1000
800
600
400
200
0
Counts
FITC-labeled particles
Control
10^0
10^1
10^2
10^3
10^4
FL1-H
B
10^4
10^3
10^2
10^1
10^0
SSC-H
R1
R2
FSC-H
C
60
40
20
0
% phagocytic cells
Zymosan
E. coli
Latex beads
D
60
50
40
30
20
10
0
% phagocytic cells
*
*
Latex beads
E. coli
Zymosan
Fractionated coelomocytes
Whole coelomocytes

Figure 3

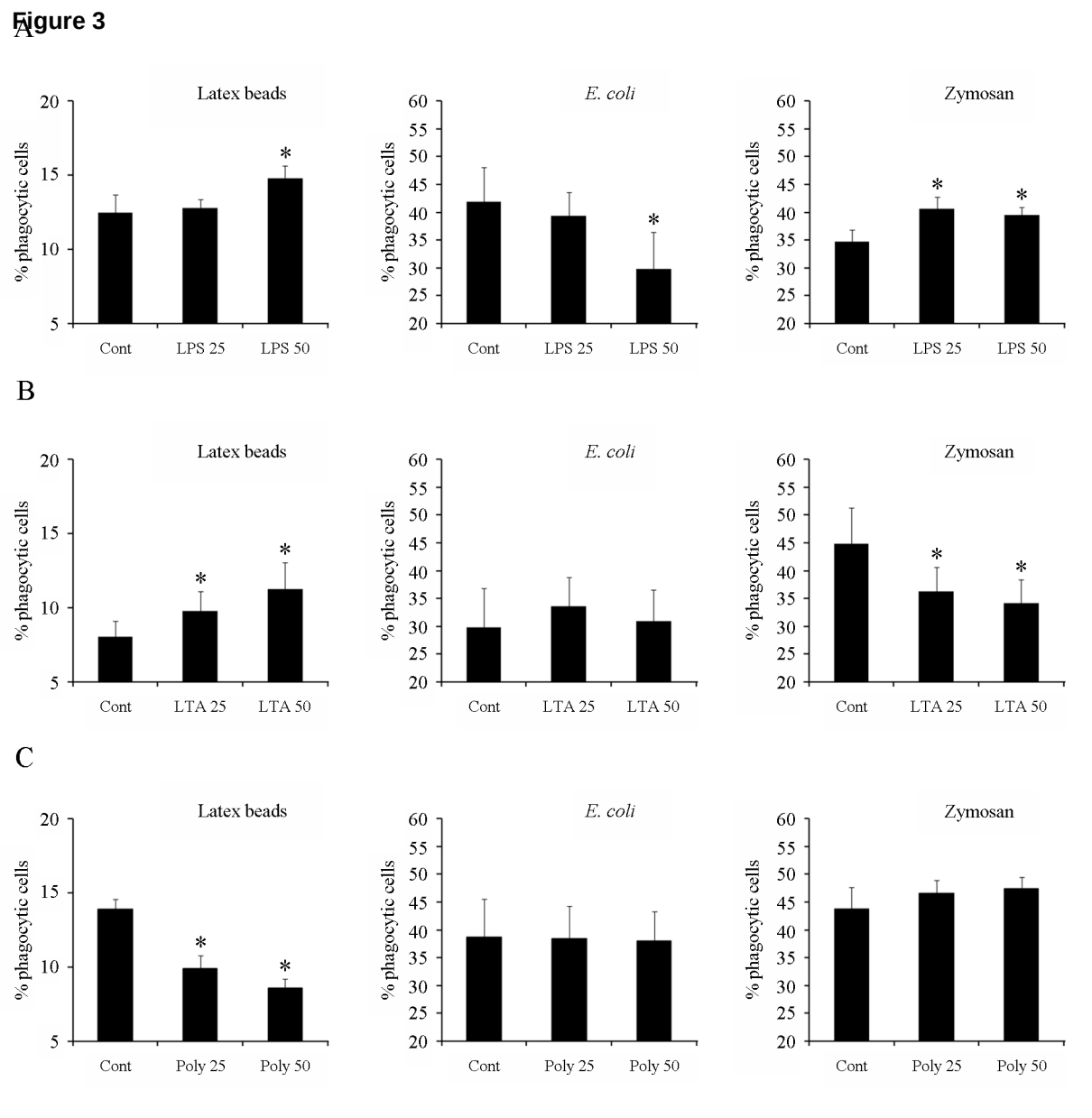
A
Latex beads
E. coli
Zymosan
% phagocytic cells
Cont
LPS 25
LPS 50
B
Latex beads
E. coli
Zymosan
% phagocytic cells
Cont
LTA 25
LTA 50
C
Latex beads
E. coli
Zymosan
% phagocytic cells
Cont
Poly 25
Poly 50

Figure 4

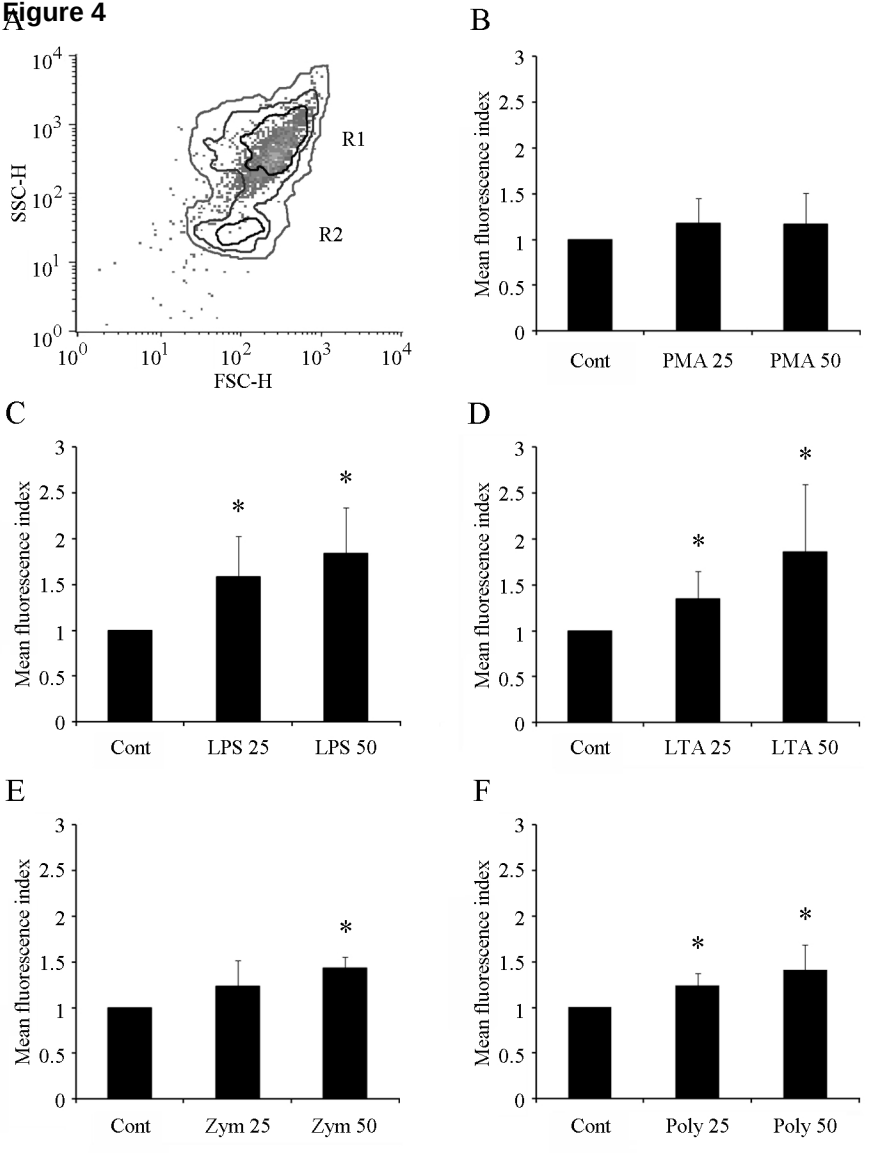
A
SSC-H
FSC-H
R1
R2
B
Mean fluorescence index
Cont
PMA 25
PMA 50
C
Mean fluorescence index
Cont
LPS 25
LPS 50
D
Mean fluorescence index
Cont
LTA 25
LTA 50
E
Mean fluorescence index
Cont
Zym 25
Zym 50
F
Mean fluorescence index
Cont
Poly 25
Poly 50

Figure 5

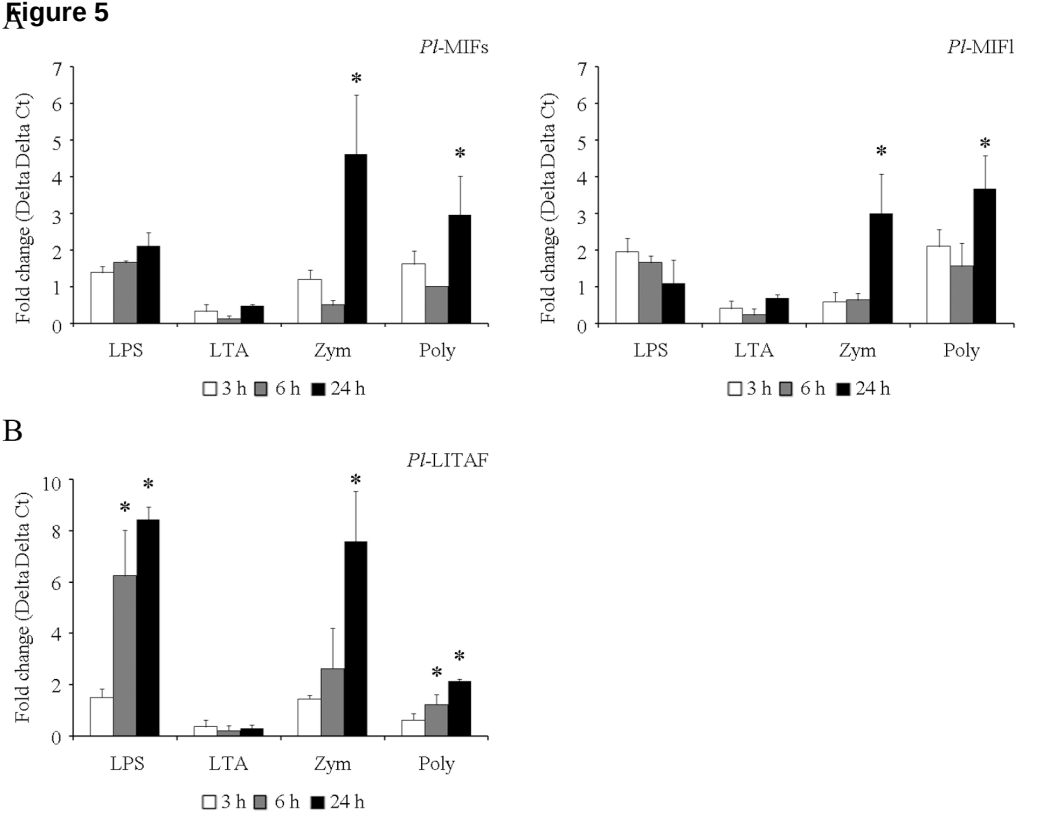
A
Pl-MIFs
Fold change (Delta Delta Ct)
0
1
2
3
4
5
6
7
*
*
LPS
LTA
Zym
Poly
3 h
6 h
24 h
Pl-MIF1
Fold change (Delta Delta Ct)
0
1
2
3
4
5
6
7
*
*
LPS
LTA
Zym
Poly
3 h
6 h
24 h
B
Pl-LITAF
Fold change (Delta Delta Ct)
0
2
4
6
8
10
*
*
*
*
*
LPS
LTA
Zym
Poly
3 h
6 h
24 h

Supplementary Figure 1

Click here to download Supplementary material for online publication only: Supplementary figure 1.pdf

Supplementary Figure 2

Click here to download Supplementary material for online publication only: Supplementary figure 2.pdf